Supplementary Information (SI) for Journal of Materials Chemistry B.
This journal is © The Royal Society of Chemistry 2025

Supporting Information

Lipopolysaccharide-Imprinted Magneto-TiO_2 Nanoagents Harness Dopamine Charge Transfer to Drive Visible-Light Photodynamic Therapy for Sepsis

Jiateng Wu, Jiali Wang, Weige Dong, Yu Wan, Chungu Zhang, Ming-Yu Wu, Shun Feng*

（Sichuan Engineering Research Center for Biomimetic Synthesis of Natural Drugs, School of Life Science and Engineering, Southwest Jiaotong University, Chengdu 610031, P. R. China）

1. Experimental Section

1.1. Materials

Tetraethyl orthosilicate (TEOS), polyethylene glycol 4000 (PEG-4000), sodium acetate (NaAc), Ethylenediaminetetraacetic acid disodium salt (EDTA), iron(III) chloride hexahydrate ($FeCl_3 \cdot 6H_2O$), 9,10-anthracenediyl-bis(methylene)dimalonic acid (ABDA), hydroxyphenyl fluorescein (HPF) and hexamethylenetetramine (HMTA) were purchased from Shanghai Aladdin Biochemical Technology Co., Ltd. (China). Tetrabutyl titanate (TBOT), fluorescein isothiocyanate isomer I (FITC), ethylene glycol, dopamine, and 3-aminophenylboronic acid (3-APBA) were purchased from Shanghai Titan Scientific Co., Ltd. (China). Lipopolysaccharide (LPS) from *Pseudomonas aeruginosa* (*P. aeruginosa*) was purchased from Sigma-Aldrich (USA). ELISA kits were purchased from Bioswamp Biotechnology Co., Ltd. (China). And CCK-8 kits were purchased from Biosharp Life Sciences Co., Ltd. (China). Ultra-pure water (18.2 MΩ cm^{-1}) was obtained with a KL-UP-II water system from Tangshi Kangning Technology Development Co., Ltd., (China) and used thoroughly in experiments. All chemical reagents were of analytical grade unless otherwise stated.

1.2 Instruments

The morphological characteristics of the nanoparticles were characterized using Fourier transform infrared spectroscopy (FT-IR; Nicolet 6700, Thermo Fisher, USA), scanning electron microscopy (SEM; JSM-7800F Prime, Japan), transmission electron microscopy (TEM; JEM-2100, JEOL Ltd., Japan), X-ray diffractometer (XRD; D8 ADVANCE, Bruker, USA), Vibrating sample magnetometry (VSM; Model 7400, Lake Shore, USA), energy dispersive spectroscopy (EDS; ISIS-2000, Oxford, UK), and UV-vis diffuse reflection spectroscopy

(UV3600, Shimadzu, Japan). Cell fluorescence intensity was analyzed using a flow cytometer (Accuri™ C6, BD Biosciences, USA). Hydrodynamic diameter and ζ-potential measurements were performed on a Zetasizer Nano ZS system (ZEN3600, Malvern Panalytical, UK). UV-Vis absorption spectra were recorded using a UV-vis spectrophotometer (UV-1800PC, AOE Instruments Co., Ltd., China) over a wavelength range of 200–800 nm.

1.3 Preparation of Fe_3O_4

Approximately 2.70 g of $FeCl_3 \cdot 6H_2O$, 7.20 g of sodium acetate (NaAc), and 2.00 g of PEG-4000 were separately dissolved in 20 mL of ethanol under ultrasonication until complete dissolution. The three solutions were then combined and magnetically stirred at 800 rpm for 30 min. Subsequently, the mixture was transferred into a poly(tetrafluoroethylene) (PTFE)-lined autoclave and reacted at 200°C for 8 h. After natural cooling to room temperature, the product was collected via magnetic separation and alternately washed with water and absolute ethanol until the supernatant reached neutral. Finally, the purified product was vacuum-dried at 50°C for 12 h.

1.4 Preparation of Fe_3O_4@SiO_2

Approximately 0.3 g of Fe_3O_4 nanoparticles (NPs) was uniformly dispersed in a mixture of 25 mL isopropanol and 5 mL deionized water under ultrasonication. Subsequently, 5 mL of ammonium hydroxide ($NH_3 \cdot H_2O$, 1 M) was added to the suspension, followed by the dropwise introduction of 2 mL tetraethyl orthosilicate (TEOS) over 10 min. The reaction mixture was mechanically stirred at 500 rpm under ambient conditions for 12 h. The resulted composite was isolated via magnetic separation and alternately washed with water and ethanol until the supernatant reached pH 7.0. Finally, the product was vacuum-dried (0.1 MPa) at 50 °C for 12 h.

1.5 Light Source Characterization and Calibration

Photoirradiation was performed using a white LED lamp (OPPLE LTG0120143001). The optical power density at the sample plane was calibrated using a certified optical power meter positioned at the target irradiation distance. The power density was calculated as:

$$Power\ Density = \frac{Total\ Lamp\ Output\ Power\ (mW)\ (mW)}{Effective\ Irradiation\ Area\ (cm^2)}$$

With measured values: Total output power = 30,000 mW (30 W), Effective irradiation area = 300 cm^2. Thus, calibrated power density is 100 $mW \cdot cm^{-2}$. This calibration methodology follows established protocols for photodynamic therapy studies.[1, 2]

2. Figure Captions

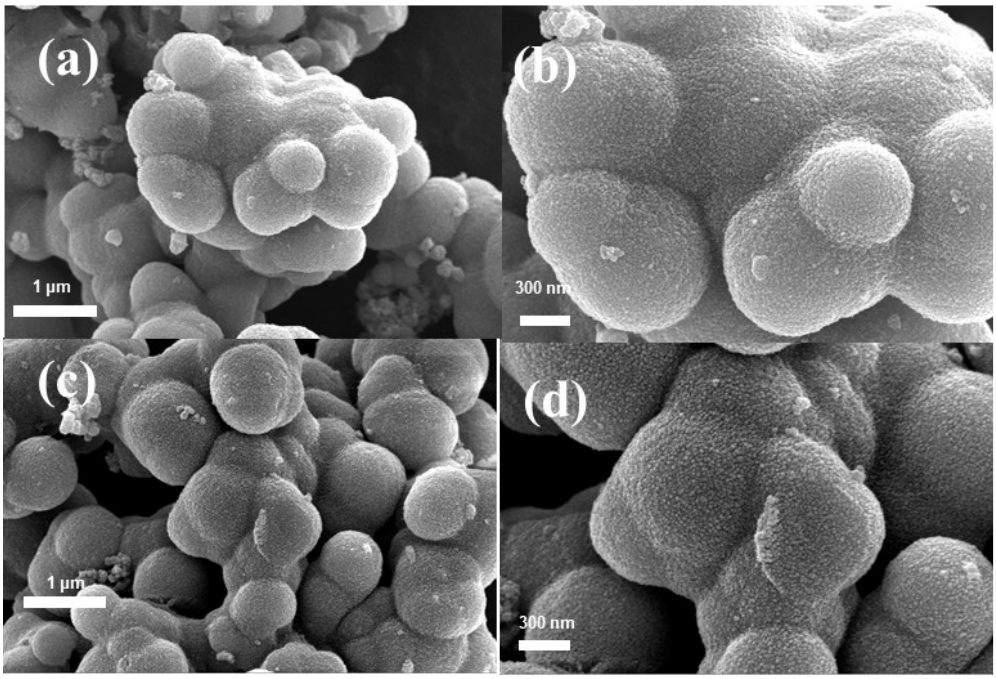

Figure S1. SEM images at low/high magnifications of (a, b) FST and (c, d) LPS-MIP microspheres.

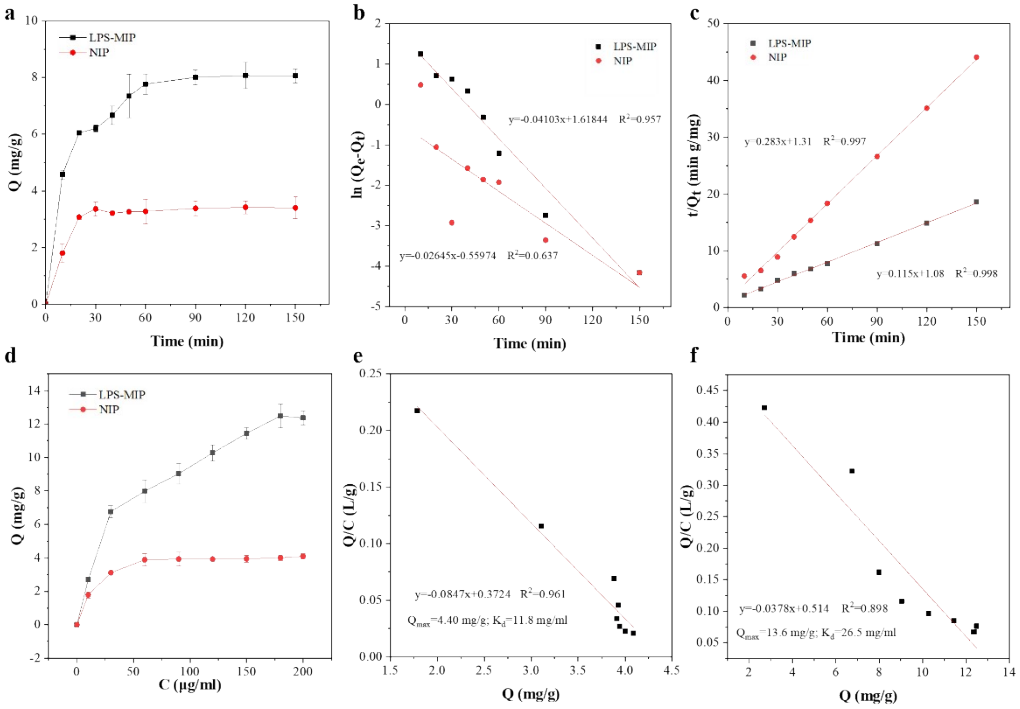

Figure S2. Dynamic adsorption curves of LPS-MIP and NIP. (a) Kinetic adsorption curve. (b) Pseudo-first-order curve. (c) Pseudo-second-order curve. (d) Isothermal adsorption curve. (e and f) Scatchard curves.

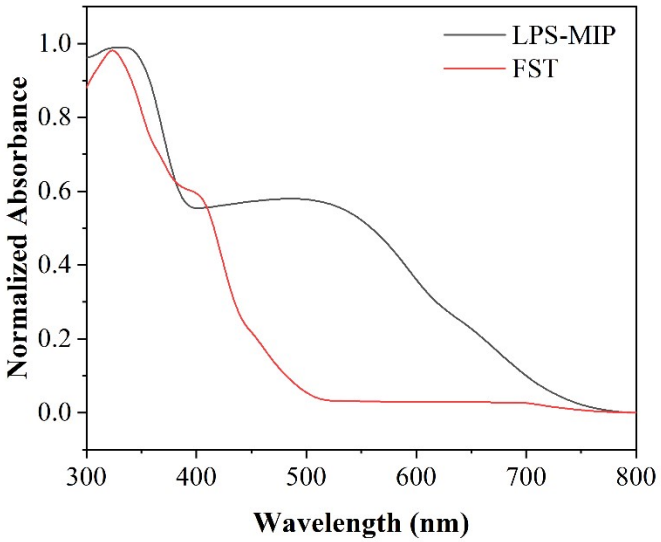

Figure S3. The UV-vis Diffuse Reflection Spectroscopy of FST and LPS-MIP.

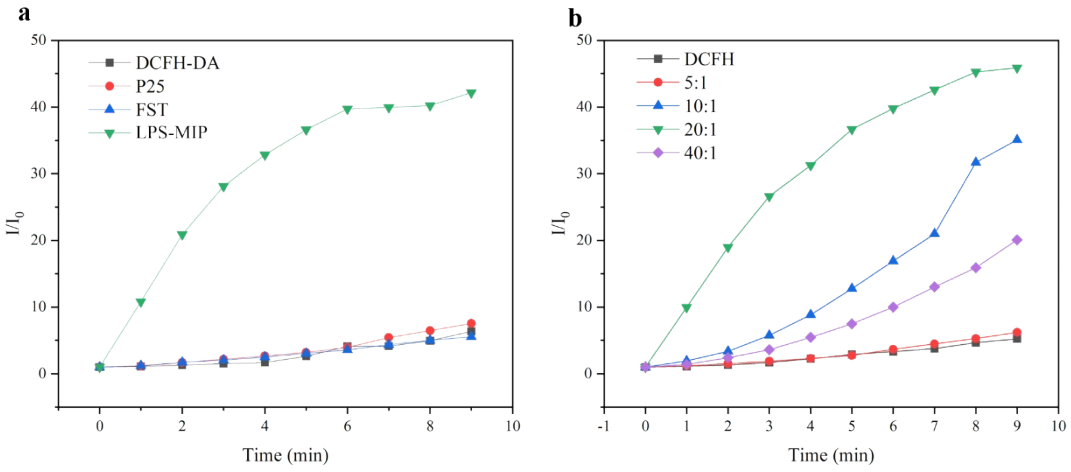

Figure S4. Fluorescence intensity changes of DCFH-DA at 525 nm under different conditions. (a) ROS generation capacity of P25, FST, and LPS-MIP upon visible-light irradiation, where I_0 and I represent the initial and final fluorescence intensities of DCFH-DA at 525 nm. (b) Concentration-dependent ROS generation capacity of LPS-MIP microspheres.

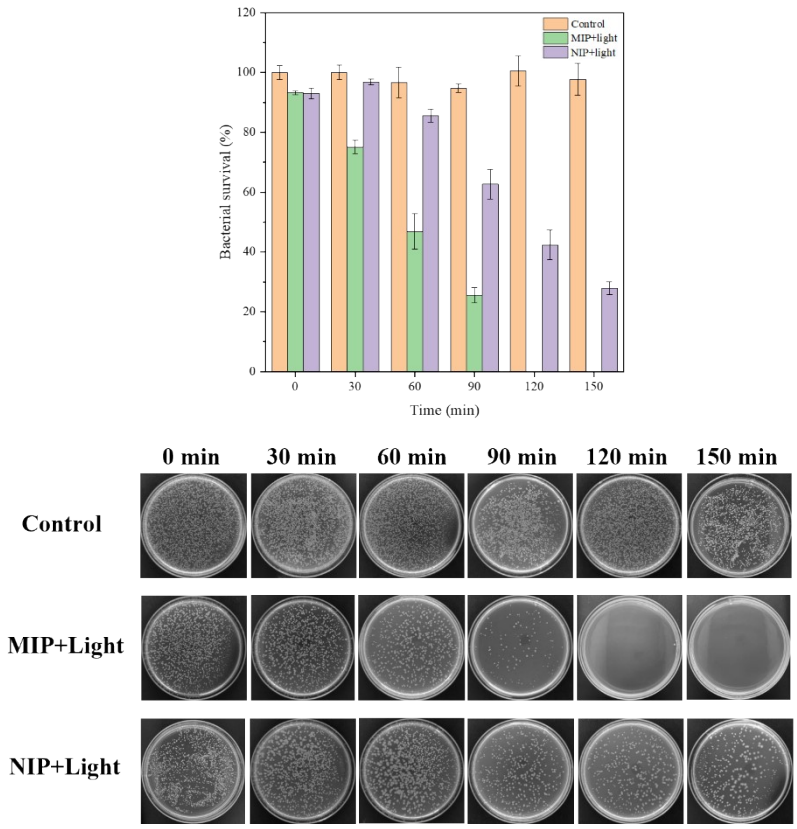

Figure S5. Survival rate of *P. aeruginosa* and corresponding plate photographs after treatment with LPS-MIP or NIP (200 μg mL^{-1}, 30 min) under *wh*ite-light irradiation for different durations.

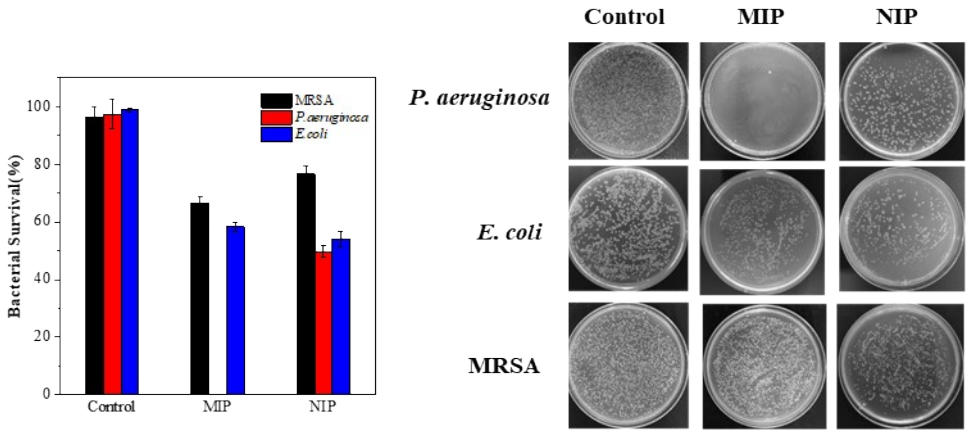

Figure S6. SEM images of *P. aeruginosa*, *E. coli*, and MRSA after treatment with LPS-MIP (200 μg mL^{-1}, 30 min) under dark conditions or with white light irradiation (120 min).

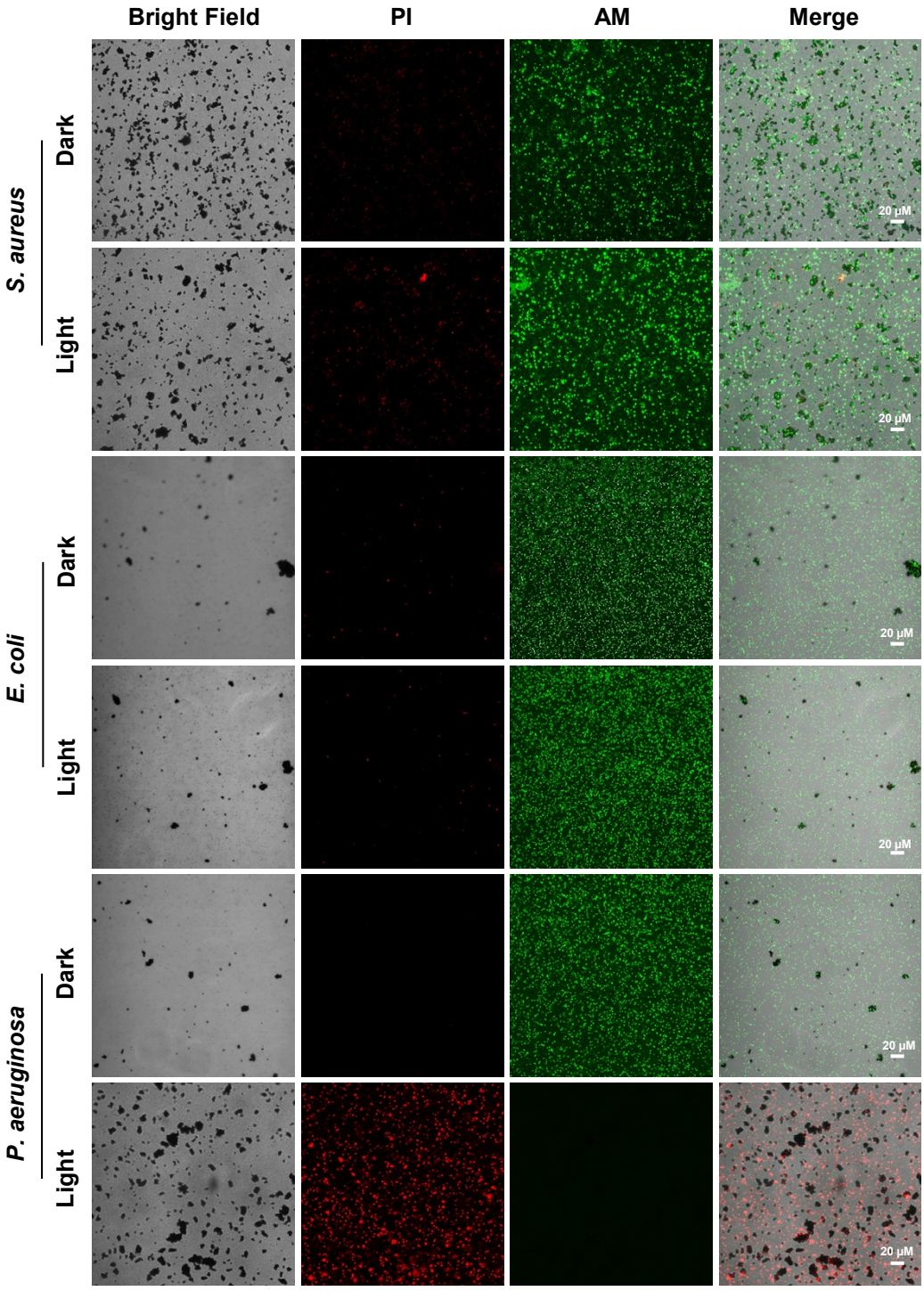

Figure S7. Live-dead fluorescence microscopy images of *P. aeruginosa*, *E. coli*, and MRSA after treatment with LPS-MIP (200 μg mL^{-1}, 30 min) under dark conditions or with white light irradiation (120 min). (Scale bars: 20 μm)

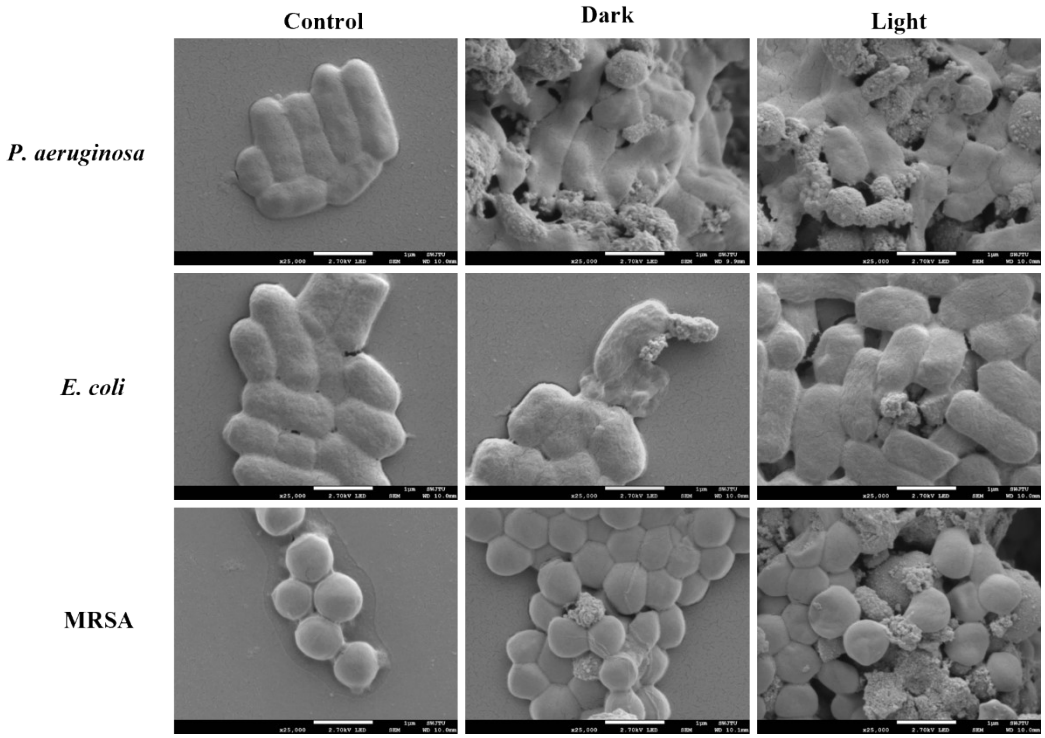

Figure S8. Representative SEM images of *P. aeruginosa*, *E. coli*, and MRSA after treatment with with LPS-MIP (200 μg mL^{-1}, 30 min) under dark conditions or with white light irradiation (120 min). (Scale bars: 1 μm)

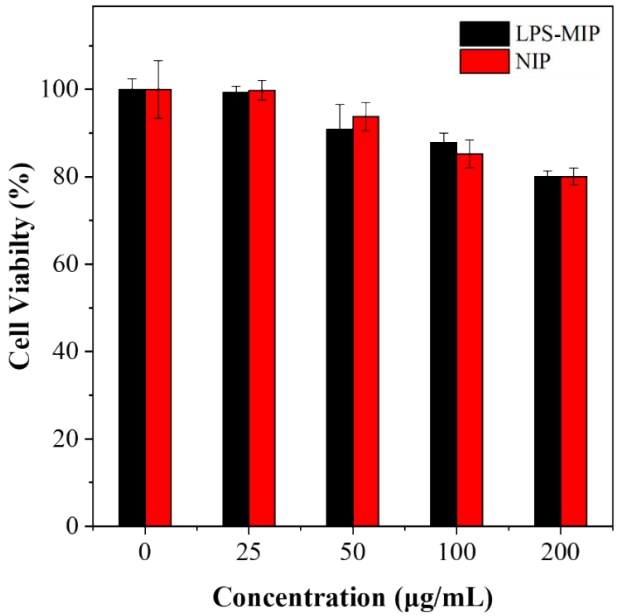

Figure S9. Viability of TC-1 cells after 24-hour incubation with varying concentrations of LPS-MIP or NIP.

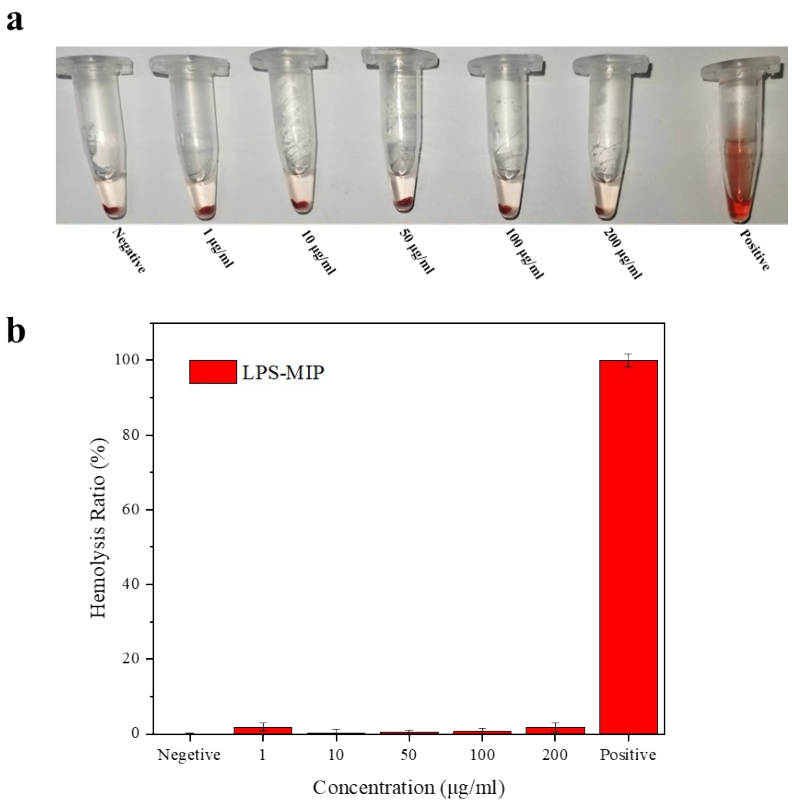

Figure S10. Hemolysis analysis of LPS-MIP. (a) Visual hemolysis assay. (b) Quantified hemolysis percentage after incubation with human red blood cells.

3. Table Captions

Table S1. Major Elemental Composition of LPS-MIP Determined by EDS Analysis.

Element	Weight %	Norm. Weight %	Atomic %]	Abs. Error (1σ) %
C	3.39	6.53	13.29	0.86
N	0.00	0.00	0.00	0.00
O	16.68	32.07	49.02	2.58
Si	11.52	22.16	19.29	0.53
Ti	8.72	16.77	8.57	0.42
Fe	11.69	22.47	9.84	0.78

Table S2. Baseline complete blood count (CBC) parameters of experimental groups on Day 1.

Inspection items	**Reference range**	**Unit**	**Control**	**PBS**	**LPS-MIP**	**Gen**
WBC	0.8~6.8	10^9 L^{-1}	2.89±0.03	2.40±0.15	2.40±0.02	2.46±0.05
NEU%	8.6~38.9	%	29.63±0.98	64.93±0.55	59.8±1.47	73.93±0.64
LYM%	55.8~90.6	%	66.87±1.80	28.53±2.11	35.7±2.02	23.93±0.42
NEU#	0.1~1.8	10^9 L^{-1}	0.86±0.04	1.56±0.1	0.24±0.02	1.82±0.06

Table S3. Baseline complete blood count (CBC) parameters of experimental groups on Day 4.

Inspection items	**Reference range**	**Unit**	**Control**	**PBS**	**LPS-MIP**	**Gen**
WBC	0.8~6.8	10^9 L^{-1}	3.47±0.09	10.57±0.23	4.35±0.03	4.43±0.07
NEU%	8.6~38.9	%	26.97±0.92	87.17±0.40	52.9±0.60	52.17±1.07
LYM%	55.8~90.6	%	70.97±1.01	11.53±0.67	45.2±0.30	45.77±1.45
NEU#	0.1~1.8	10^9 L^{-1}	0.94±0.05	9.21±0.18	2.30±0.03	2.31±0.01

Table S4. Comparative hematological parameters of control and LPS-MIP-treated groups at Day 7 post-treatment. (Data presented as mean ± SD; n = 3 per group)

Inspection items	Reference range	Unit	PBS	LPS-MIP
WBC	0.8~6.8	10^9 L^{-1}	3.37±0.010	3.99±0.11
RBC	6.36~9.42	10^{12} L^{-1}	11.13±0.10	9.66±0.62
HGB	110~143	g L^{-1}	173.33±3.51	147.00±7.00
MCV	48.2~58.3	fL	61.83±0.95	55.43±0.31
PLT	450~1590	10^9 L^{-1}	450.00±20.66	615.00±118.65
NEU%	8.6~38.9	%	29.70±1.8	28.83±0.91
LYM%	55.8~90.6	%	66.47±1.8	67.07±0.81
MON%	1.8~6	%	3.57±3.57	2.90±0.46
EOS%	3.6~13	%	0.10±0.00	0.23±0.12
BAS%	0.7~5.1	%	0.17±0.06	0.97±0.29
NEU#	0.1~1.8	10^9 L^{-1}	1.34±0.06	1.15±0.07
LYM#	0.7~5.7	10^9 L^{-1}	1.91±0.06	2.67±0.05
MON#	0~0.3	10^9 L^{-1}	0.12±0.01	0.12±0.02
EOS#	0~0.6	10^9 L^{-1}	0.00±0.00	0.01±0.01
BAS#	0~0.2	10^9 L^{-1}	0.01±0.01	0.04±0.01
HCT	34.6~44.6	%	68.87±1.51	53.57±3.71
MCH	15.8~19	pg	15.57±0.29	15.20±0.26
MCHC	302~353	g L^{-1}	252.00±7.55	274.67±6.35
RDW-CV	11~17	%	11.67±0.15	10.80±0.00
RDW-SD	33~50	fL	26.43±0.92	22.80±1.04
MPV	3.8~6	fL	17.70±0.10	14.00±0.82
PCT	0~0.3	%	0.80±0.03	0.86±0.12
PDW	0~18	-	22.20±0.10	21.67±0.06
P-LCR	0.13~0.43	-	0.70±0.01	0.46±0.05
P-LCC	10~100	10^9 L^{-1}	316.00±8.72	278.33±28.02

1 J. M. Elson and J. M. Bennett, *Appl Opt*, 1995, **34**, 201-208.

2 A. François, A. Salvadori, A. Bressenot, L. Bezdetnaya, F. Guillemin and M. A. D'Hallewin, *J Urology*, 2013, **190**, 731-736.